ISSN 1674-1056
http://cpb.iphy.ac.cn
http://iopscience.iop.org/cpb
中国物理 B
Chinese Physics
中国物理
Chinese Physics B

Non-crossover sub-Doppler DAVLL in selective reflection scheme

Lin-Jie Zhang(张临杰), Hao Zhang(张好), Yan-Ting Zhao(赵延霆), Lian-Tuan Xiao(肖连团), Suo-Tang Jia(贾锁堂)

Citation: Chin. Phys. B . 2019, 28(8): 084211 . **doi:** 10.1088/1674-1056/28/8/084211
Journal homepage: http://cpb.iphy.ac.cn; http://iopscience.iop.org/cpb

What follows is a list of articles you may be interested in

Active hyperspectral imaging with a supercontinuum laser source in the dark

Zhongyuan Guo(郭中源), Yu Liu(刘煜), Xin Zheng(郑鑫), Ke Yin(殷科)
Chin. Phys. B . 2019, 28(3): 034206 . **doi:** 10.1088/1674-1056/28/3/034206

Nonlinear behavior of the population dynamics of three-level systems in the presence of single photon absorption

Allam Srinivasa Rao
Chin. Phys. B . 2019, 28(2): 024211 . **doi:** 10.1088/1674-1056/28/2/024211

Laser absorption spectroscopy for high temperature H_2O time-history measurement at 2.55 μm during oxidation of hydrogen

Yu-Dan Gou(苟于单), De-Xiang Zhang(张德翔), Yi-Jun Wang(王易君), Chang-Hua Zhang(张昌华), Ping Li(李萍), Xiang-Yuan Li(李象远)
Chin. Phys. B . 2018, 27(7): 074213 . **doi:** 10.1088/1674-1056/27/7/074213

Analysis of algebraic reconstruction technique for accurate imaging of gas temperature and concentration based on tunable diode laser absorption spectroscopy

Hui-Hui Xia(夏晖晖), Rui-Feng Kan(阚瑞峰), Jian-Guo Liu(刘建国), Zhen-Yu Xu(许振宇), Ya-Bai He(何亚柏)
Chin. Phys. B . 2016, 25(6): 064205 . **doi:** 10.1088/1674-1056/25/6/064205

Lasing dynamics study by femtosecond time-resolved fluorescence non-collinear optical parametric amplification spectroscopy

Wei Dang(党伟), Qing Liao(廖清), Peng-Cheng Mao(毛鹏程), Hong-Bing Fu(付红兵), Yu-Xiang Weng(翁羽翔)
Chin. Phys. B . 2016, 25(5): 054207 . **doi:** 10.1088/1674-1056/25/5/054207

Non-crossover sub-Doppler DAVLL in selective reflection scheme*

Lin-Jie Zhang(张临杰)[1,2], Hao Zhang(张好)[1,2], Yan-Ting Zhao(赵延霆)[1,2,†], Lian-Tuan Xiao(肖连团)[1,2], and Suo-Tang Jia(贾锁堂)[1,2]

[1] State Key Laboratory of Quantum Optics and Quantum Optics Devices, Institute of Laser Spectroscopy, Shanxi University, Taiyuan 030006, China

[2] Collaborative Innovation Center of Extreme Optics, Shanxi University, Taiyuan 030006, China

(Received 20 March 2019; revised manuscript received 6 May 2019; published online 25 July 2019)

We demonstrate a non-crossover sub-Doppler dichroic atomic vapor laser locking (DAVLL) in selective reflection scheme, which allows us to obtain a modulation-free laser locking with wide tuneable range. The dependence of peak-to-peak amplitude, tuneable range and the slope near the zero-crossing point of error signal on the frequency shift induced by the magnetic fields are studied. The adjustable error signal by the varying external magnetic field can offer the laser locking from the order of tens MHz to hundreds MHz. The ultimate dither of locked laser frequency is less than 0.5 MHz. The square root of Allan variance of the error signals reaches a minimum of 3×10^{-10} for an averaging time of 130 s.

Keywords: reflection spectrum, DAVLL, sub-Doppler frequency stabilization

PACS: 42.62.Fi, 78.40.–q, 32.10.Fn, 32.30.–r **DOI:** 10.1088/1674-1056/28/8/084211

1. Introduction

The appearance of external cavity diode lasers extremely accelerates the development of atomic physics, quantum optics, and laser spectroscopy.[1] A common issue of laser is frequency fluctuation mainly induced by mechanical vibration and temperature drift of laser diode. In the past decades, numerous schemes have been proposed to stabilize laser frequency to atomic transition lines. The conventional technique employs saturated absorption spectroscopy (SAS) with frequency modulation to get the error signal.[2] This technique cannot avoid the extra frequency modulation added to the laser output. Therefore, lots of modulation-free schemes are proposed to lock laser frequency, such as polarization spectroscopy,[3,4] light-induced birefringence spectroscopy,[5] and low-field Faraday polarimetry.[6] A modulation-free technique called dichroic atomic vapor laser locking (DAVLL)[7] is also developed. One advantage of DAVLL is the frequency offset of locked laser from the atomic transition line can be controlled by laser beam polarization.[8] The other advantage is large frequency capture range induced by Doppler background.[7,9] But the Doppler background simultaneously brings some disadvantages, the low frequency resolution and the requiring of strong magnetic field. To overcome them, a sub-Doppler DAVLL scheme is recently developed to stabilize laser frequency.[10–12] That technique combines the advantages of SAS and DAVLL, and allows us to lock laser frequency to atomic resonance lines and crossovers without modulation. However, we sometimes need to eliminate the effect of crossover in high-resolution spectroscopy.[13] When the level spacing of hyperfine structures is of the order of one or two natural linewidth, the crossover resonance often swamps the real peaks and makes it impossible to resolve the two transitions. In selective reflection scheme, the longitudinal atomic velocity is approximately zero when atoms collision with cell interface, thus the crossover peak does not exist comparing with SAS.[14,15] It is a natural idea to combine the DAVLL method with reflection spectrum to stabilize laser frequency at only resonance transition without modulation.

In this work, we demonstrate the application of sub-Doppler DAVLL in selective reflection scheme of Rb atom vapor. Through the theoretical simulation and experiment, we investigate the dependence of peak-to-peak amplitude, capture range and the slope near the zero-crossing point of error signal on the strength of magnetic field. We choose a proper strength of magnetic field and employ the error signal to lock the laser frequency. The locked frequency dither is less than 0.5 MHz, and the frequency drift is significantly suppressed, which demonstrates the effectiveness of this technique in frequency stabilization.

2. Simplified theoretical model

The resonance reflection at the interface between glass cell wall and atomic vapor was firstly discovered in 1909.[16] This effect is known as selective reflection with sub-Doppler structure at the atomic absorption line. The selective reflection arises from combinations of the effects of velocity dependent transient behavior and the nonlinear response of atoms.[17]

On the condition of normal incident, the line shape of selective reflection from the low density vapor $N \ll (\lambda/2\pi)^{-3}$ in two-level system is[18]

$$R(y \equiv \frac{\omega - \omega_0}{\Gamma_D}) \propto \mathrm{Re} \int_0^\infty \frac{\mathrm{e}^{-u^2}}{(u-y) - \mathrm{i}\gamma/2\Gamma_D} \mathrm{d}u. \quad (1)$$

*Project supported by the National Key Research and Development Program of China (Grant Nos. 2017YFA0304203 and 2016YFF0200104), the National Natural Science Foundation of China (Grant No. 61827824), the Fund from the BAIREN Plan of Shanxi Province, China, and the Funding for Shanxi "1331 Project" Key Subjects Construction, China.

†Corresponding author. E-mail: zhaoyt@sxu.edu.cn

© 2019 Chinese Physical Society and IOP Publishing Ltd

Here, γ is the homogeneous width, ω is the laser frequency, ω_0 is the frequency on the resonance, u is the reduced velocity indicated by $v\sqrt{m/(2kT)}$, v is the hot atoms velocity, and $\Gamma_{\rm D} = 2\omega_0\sqrt{2kT\ln 2/(mc^2)}$ is the full-width at half maximum amplitude of the Doppler width, where T is the absolute temperature, k is the Boltzmann constant, m is the atomic mass, and c is the velocity of light. The line shape of selective reflection expressed in Eq. (1) arises from the polarization collisions between the atoms and the dielectric interface.

In weak magnetic field or linear Zeeman splitting regime, the hyperfine level splitting can be written as

$$\Delta E_{|F,m_{\rm F}\rangle} = \mu_{\rm B} g_{\rm F} m_{\rm F} B_Z, \tag{2}$$

where $g_{\rm F}$ is hyperfine Landég-factors which is given by the relation $g_{\rm F} \simeq g_J[F(F+1) - I(I+1) + J(J+1)/2F(F+1)]$ with the nuclear term neglected, $m_{\rm F}$ is the number of Zeeman sublevel, $\mu_{\rm B}$ is Bohr magneton, and B_Z is the strength of magnetic field. From Eq. (2), we can find that the energy shift of each hyperfine level is proportional to the strength of magnetic field. The resonance peak of σ^+ (or σ^-) component of selective reflection is composed by $2F+1$ hyperfine transitions. To simplify the calculation, it is normal to regard hyperfine components with the same polarized transition as one transition. That means the hyperfine number of ground state F is zero while the value of excited state F' is one. Therefore, we can get the error signal through a subtraction of two circularly polarized components, whose line shape can be represented by Eq. (1). The line shape of error signal can be written as

$$S(y \equiv \frac{\omega-\omega_0}{\Gamma_{\rm D}}) \propto {\rm Re}\int_0^\infty \frac{{\rm e}^{-u^2}}{(u-y-\delta)-{\rm i}\gamma/2\Gamma_{\rm D}}{\rm d}u - {\rm Re}\int_0^\infty \frac{{\rm e}^{-u^2}}{(u-y+\delta)-{\rm i}\gamma/2\Gamma_{\rm D}}{\rm d}u, \tag{3}$$

where δ is the frequency shift from one circularly polarized transition component of selective reflection spectra in presence of magnetic field. The corresponding transition possibilities of two circularly polarized transition components are set to the same value in default. Figure 1 shows the simulated consequence of DAVLL error signals with different frequency shift δ in selective reflection. In simulation the homogeneous width γ contains the natural linewidth (6 MHz for D_2 line) and collisional width (15 MHz).[19] Doppler width $\Gamma_{\rm D}$ for Rb atoms at the temperature of 160 °C equals 620 MHz. However, it is shown in the inset of Fig. 1 that the locking point shift with the changing frequency shift δ will result in the uncertainty of locking frequency. To precisely determine the locking frequency, the offset of DAVLL signal can be adjusted according to the calculated locking shift to eliminate the influence from the locking point shift.

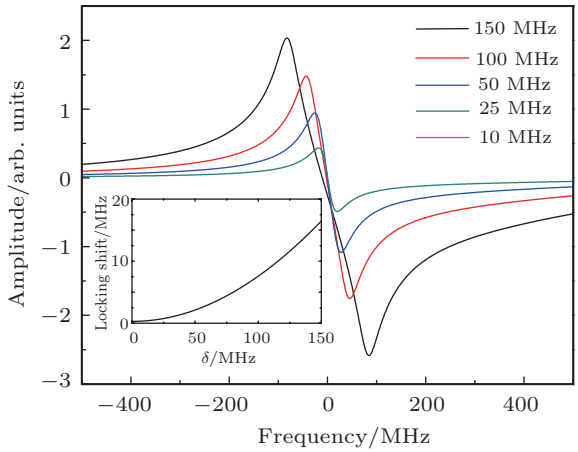


Fig. 1. Simulation of DAVLL error signals in selective reflection after simplifying the several magnetic sublevel transitions as two circularly polarized transition components, in which the frequency shifts δ are set as 10, 25, 50, 100, 150 MHz, respectively. The inset shows the relationship between the locking point shift and δ.

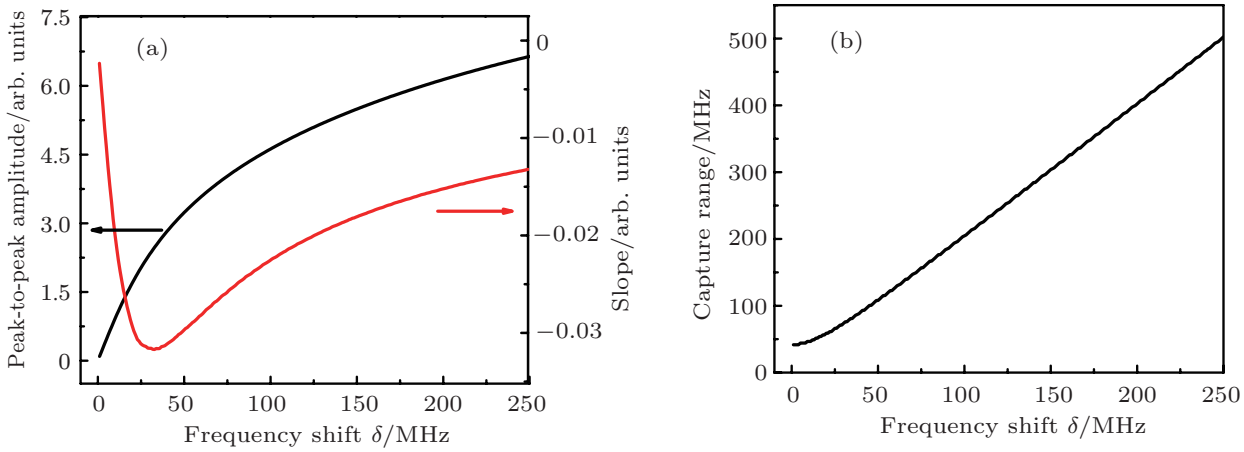


Fig. 2. (a) Dependence of peak-to-peak amplitude (black line) and the slope (red line) of the simulated error signal on the frequency shift. (b) Dependence of capture range on the frequency shift.

The corresponding peak-to-peak amplitude and the slope near the zero-crossing point as a function of frequency shift are shown in Fig. 2(a). The amplitude of error signal increases as the frequency shift increases and reaches saturation gradually. The slope has an extreme value and it reveals the sensitivity of servo system to the frequency dither induced by external

perturbation. The extreme value of the slope implies the best strength of magnetic field to lock laser frequency. The magnetic field can change frequency shifts of σ^+ and σ^- components, then the capture range. It is related to the frequency excursion that the system can tolerate and still return to the desired lock-point, and roughly equals to 2δ. Figure 2(b) shows the dependence of capture range of this locking method on the frequency shift δ. We find that the capture range is almost proportional to frequency shift. Thus, controlling the locked frequency is possible through changing the strength of external magnetic field within the reasonable range. It is an important feature for physical experiments such as atomic traps.

3. Experiment and results

Figure 3 shows the experimental setup. External cavity diode laser (New Focus, 6017) emits 780-nm beam with the diameter of approximately 2 mm. The SAS is used as a frequency reference. The vapor cell is heated to 160 °C and the corresponding pressure is approximately 7×10^{-3} Torr (1 Torr = 1.33322×10^2 Pa). The reflection window is designed to be wedged to split the lights from glass–air interface and glass–atom interface, for increasing the signal-to-noise ratio of reflection spectrum. The power of incident beam is about 1.5 μW. Two coils generate a uniform magnetic field along light direction. The two circularly polarized components of reflected light are converted to two linear polarized lights after a quarter waveplate and a polarizing beam splitter (PBS). By subtracting and amplifying the two signals, we can get the DAVLL spectrum which can be used as an error signal to stabilize the laser frequency.

Figure 4(a) shows the sub-Doppler DAVLL signal related to the transitions $F = 3 \rightarrow F'$ of ^{85}Rb D_2 line with magnetic field of 16.9 Gs (1 Gs = 10^{-4} T). Figure 4(b) shows the case related to the transitions $F = 2 \rightarrow F'$ of ^{87}Rb D_2 line with magnetic field of 12.7 Gs. The blue lines are the DAVLL signals and the green lines are the SAS for frequency reference without the magnetic fields. The hyperfine transitions and crossover transitions of ^{85}Rb and ^{87}Rb D_2 lines are labeled with arrows in SAS spectrum. Comparing the two spectra, it is obvious that there is no crossover in DAVLL spectrum. Because the DAVLL signal is obtained from the spectra reflected by the atomic interface near the glass cell, it is immune to the crossover effect arising from the atomic opposite motion. In Fig. 4, the DAVLL signals have asymmetric dispersion-like shape, which is an important feature produced by the difference of energy shift and the transition probability of each magnetic sublevel between σ^+ and σ^- resonance transition. The sign of the slope is decided by the direction of energy shift of each magnetic sublevel due to Zeeman effect.

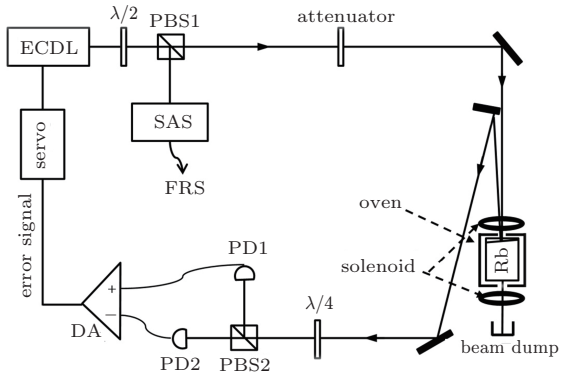


Fig. 3. Schematic diagram of sub-Doppler DAVLL signals of selective reflection in atomic rubidium. ECDL: external cavity diode laser; SAS: saturated absorption spectroscopy; PBS: polarizing beam splitter; FRS: frequency reference signal; PD: photodiode detector; DA: differential amplifier.

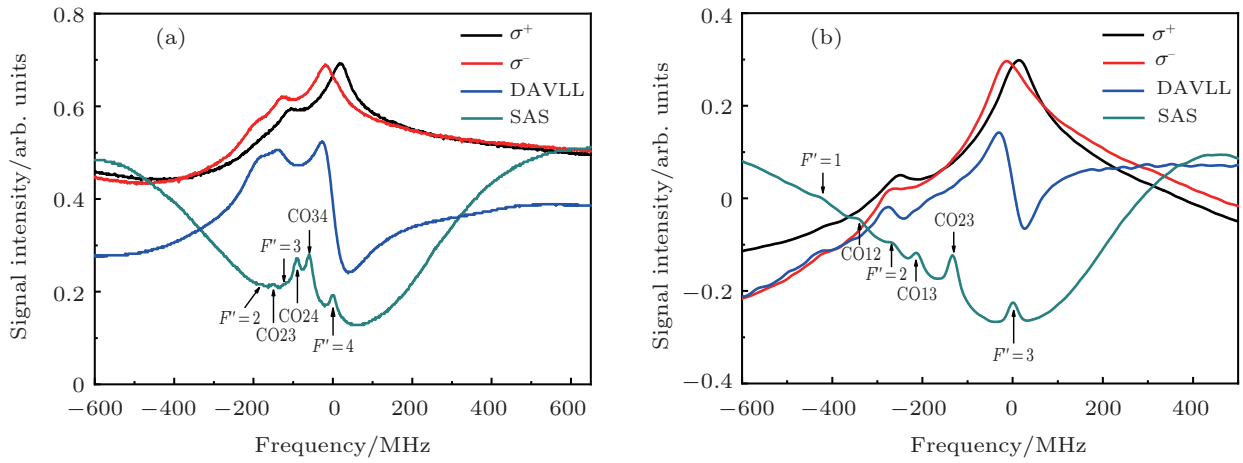


Fig. 4. Sub-Doppler DAVLL signals in selective reflection scheme with magnetic fields and saturate absorption spectroscopy signals without magnetic fields. (a) The signals are related to the transitions of ^{85}Rb D_2 line. The black and red lines represent respectively the σ^+ and σ^- polarized components of reflected spectrum of $F = 3$ to $F' = 4$ transition with magnetic field of 16.9 Gs. The green line represents saturate absorption spectroscopy signals, in which $F' = 2$, $F = 3$, and $F' = 4$ show the transition of $F = 3$ to $F' = 2, 3, 4$ and CO23, CO24, CO34 mean the transition to 2–3, 2–4, and 3–4 crossover. (b) The signals are related to the transitions of ^{87}Rb D_2 line. The black and red lines represent respectively the σ^+ and σ^- polarized components of reflected spectrum of $F = 2$ to $F' = 3$ transition with magnetic field of 12.7 Gs. The green line represents saturate absorption spectroscopy signals, in which $F' = 1$, $F' = 2$, and $F' = 3$ show the transition of $F = 2$ to $F' = 1, 2, 3$, and CO12, CO13, CO23 mean the transition to 1–2, 1–3, and 2–3 crossover. The blue curve is the DAVLL signal.

Figure 5 shows the dependence of peak-to-peak amplitudes (black squares) and slopes (red triangles) near the zero-crossing points of DAVLL signals on the strength of magnetic field. In Fig. 5(a), for the transition $F = 3 \rightarrow F' = 4$ of ^{85}Rb D_2 line, the amplitude of DAVLL signal increases as the frequency shift increases and reaches saturation gradually. The effectiveness of frequency lock significantly depends on the slope of error signal. The red triangle shows the corresponding ratio obtained from amplitude divided by the corresponding capture range. The slope is negative and has an extreme value at magnetic field of about 30 Gs. In Fig. 5(b), for the transition $F = 2 \rightarrow F' = 3$ of ^{87}Rb D_2 line, we obtain the analogous property.

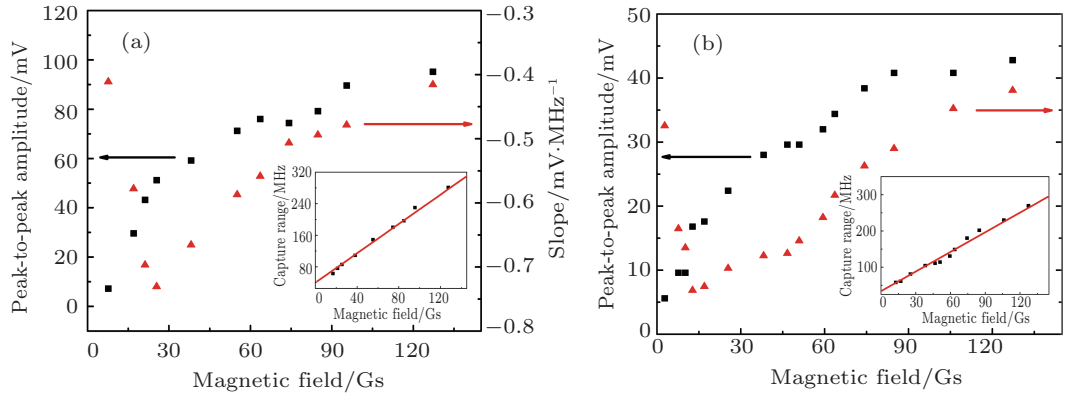


Fig. 5. Dependence of peak–peak amplitude (black squares) and slope (red triangles) of error signal on the strength of magnetic field. (a) $F = 3 \rightarrow F' = 4$ of ^{85}Rb D_2 line. (b) $F = 2 \rightarrow F' = 3$ of ^{87}Rb D_2 line. The insets show the dependence of capture range on the strength of magnetic field.

The insets of Fig. 5 show the dependence of capture range on the strength of magnetic field for the transitions $F = 3 \rightarrow F' = 4$ of ^{85}Rb D_2 line and $F = 2 \rightarrow F' = 3$ of ^{87}Rb D_2 line, respectively. The capture range is proportional to the strength of magnetic field and agrees with the simulation. The ratio of capture range to magnetic field is about 1.86 MHz/Gs and 1.81 MHz/Gs for ^{85}Rb and ^{87}Rb respectively. Owing to the relative wide capture range controlled by magnetic field, we can use it to choose the desired frequency through adjusting the offset of discriminant line. It is an important feature for tuning the locked laser frequency relative to resonance line in some experiments, such as atom trapping in magneto–optical traps. Comparing with Fig. 2(a), the similar saturation effects of the DAVLL amplitudes are observed in both Fig. 5(a) and Fig. 5(b) with the magnetic field about 120 Gs. The slope of DAVLL signal presents a minimum with the magnetic field 28 Gs in Fig. 5(a) and the magnetic field about 15 Gs in Fig. 5(b).

Figure 6(a) shows the results with and without the servo loop at a fixed magnetic field of 30 Gs for the transition $F = 3 \rightarrow F' = 4$ of ^{85}Rb D_2 line. The frequency drift is approximately 10 MHz from the zero-crossing point of error signal in 200 s. After switching on the servo loop, the frequency fluctuation is confined less than 0.5 MHz. For the long term drift of locking frequency, it would be helpful to make the magnetic field. and temperature stable for the vapor cell. The corresponding square root of Allan variance is calculated and shown in Fig. 6(b). It reaches the minimum 3×10^{-10} at averaged time of 130 s. For the free running diode laser, the minimum value is 1×10^{-9} at 4 s. Through the square root of Allan variance, we find that the laser obtains a stabilization improvement by sub-Doppler DAVLL in selective reflection scheme. It demonstrates the effectiveness of this method in suppressing laser frequency drift and fluctuation noise.

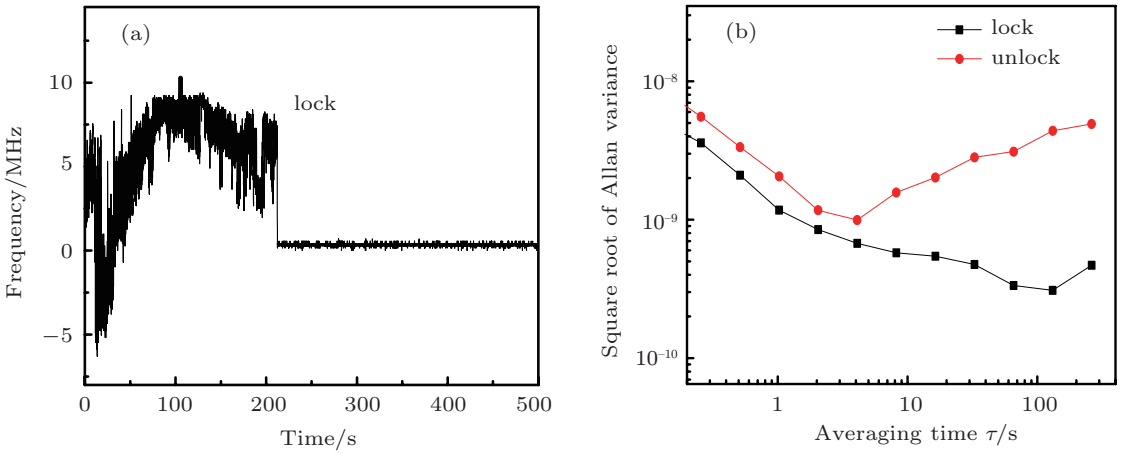


Fig. 6. (a) The error signal with and without feedback from a DAVLL selective reflection spectra for the transition $F = 3 \rightarrow F' = 4$ of ^{85}Rb D_2 line. (b) Square root of Allan variance with and without locking for the laser frequency.

4. Conclusion

We have demonstrated the sub-Doppler DAVLL in selective reflection scheme with the wider tunable frequency range and free-modulation. The dependence of peak-to-peak amplitude, capture range and the slope near the zero-crossing point of error signal on frequency shift induced by magnetic field is studied through theoretical simulation and experiment. In the linear Zeeman effect regime, we find the amplitude of error signal is close to saturation when the frequency shift of two circularly polarized components is big enough. The slope has an extreme value for the variation of frequency shift. Ultimately, this error signal is used to lock laser frequency and the frequency fluctuations is successfully confined less than 0.5 MHz. The calculated square root of Allan variance demonstrates the feasibility of frequency stabilization using this scheme.

Comparing with conventional laser stabilization scheme, such as modulated SAS, the sub-Doppler DAVLL in selective reflection scheme has several advantages besides the free modulation. First, a weak laser intensity with the order of microwatt can offer the good signal-to-noise ratio of DAVLL signal because of the high atomic density on the reflective surface. As a result, the energy shift induced by the laser intensity can be ignored. Second, there is no crossover in the selective reflection spectrum, which is very important in high-resolution spectroscopy. Furthermore, the capture range can be controlled from the order of tens MHz to hundreds MHz by justly changing the magnetic field. It can be easily achieved great improvement of the signal-to-noise ratio of error signal by heating the vapor cell. On the other hand, the locking frequency point is moderate sensitive(0.14 kHz/K) to the temperature. In conclusion, the sub-Doppler DAVLL in selective reflection scheme can realize the wide tunable locking frequency range with the lower laser power consumption and compact optical module.

References

[1] Nasim H and Jamil Y 2013 *Laser Phys. Lett.* **10** 043001
[2] Hori H, Kitayama Y, Kitano M, Yabuzaki T and Ogawa T 1983 *IEEE J. Quantum Electron.* **19** 169
[3] Wieman C and Hänsch T W 1976 *Phys. Rev. Lett.* **36** 1170
[4] Pearman C P, Adams C S, Cox S G, Griffin P F, Smith D A and Hughes I G 2002 *J. Phys. B: At., Mol. Opt. Phys.* **35** 5141
[5] Yoshikawa Y, Umeki T, Mukae T, Torii Y and Kuga T 2003 *Appl. Opt.* **42** 6645
[6] Kerckhoff J A, Bruzewicz C D, Uhl R and Majumder P K 2005 *Rev. Sci. Instrum.* **76** 093108
[7] Corwin K L, Lu Z T, Hand C F, Epstein R J and Wieman C E 1998 *Appl. Opt.* **37** 3295
[8] Wasik G, Gawlik W, Zachorowski J and Zawadzki W 2002 *Appl. Phys. B* **75** 613
[9] Yin S, Liu H, Qian J, Hong T, Xu Z and Wang Y 2012 *Opt. Commun.* **285** 5169
[10] Harris M L, Cornish S L, Tripathi A and Hughes I G 2008 *J. Phys. B: At., Mol. Opt. Phys.* **41** 085401
[11] Pichler M and Hall D C 2012 *Opt. Commun.* **285** 50
[12] Su D Q, Meng T F, Ji Z H, Yuan J P, Zhao Y T, Xiao L T and Jia S T 2014 *Appl. Opt.* **53** 7011
[13] Banerjee A and Natarajan V 2003 *Opt. Lett.* **28** 1912
[14] Zhao J M, Zhao Y T, Wang L R, Xiao L T and Jia S T 2002 *Appl. Phys. B* **75** 553
[15] Li R N, Jia S T, Bloch D and Ducloy M 1998 *Opt. Commun.* **146** 186
[16] Wood R 1909 *Philosophical Magazine Series 6* **18** 187
[17] Schuller F, Nienhuis G and Ducloy M 1991 *Phys. Rev. A* **43** 443
[18] Burgmans A L J and Woerdman J P 1976 *J. Phys. France* **37** 677
[19] Kondo R, Tojo S, Fujimoto T and Hasuo M 2006 *Phys. Rev. A* **73** 062504